Adsorption of Bovine Serum Albumin on Chromium and Molybdenum Surfaces Investigated by Fourier-Transform Infrared Reflection−Absorption Spectroscopy (FT-IRRAS) and X-ray Photoelectron Spectroscopy

C. M. Pradier,*,† F. Kármán,‡ J. Telegdi,‡ E. Kálmán,‡ and P. Marcus*,†

Laboratoire de Physico-Chimie des Surfaces, CNRS (UMR 7045), Ecole Nationale Supérieure de Chimie de Paris, 11 rue P. et M. Curie, 75005 Paris, France, and Chemical Research Center, Department of Surface Chemistry and Corrosion Research, Hungarian Academy of Sciences, H-1025 Budapest, Hungary

Received: June 24, 2002; In Final Form: April 1, 2003

The adsorption of bovine serum albumin (BSA) was investigated on two metal surfaces, chromium and molybdenum, in pure water and in a phosphate buffer solution (pH 7). Fourier-transform infrared reflection−absorption spectroscopy (FT-IRRAS) and X-ray photoelectron spectroscopy (XPS) were used to characterize the surfaces after immersion times ranging from 2 min to 1 h. In pure water, short times of immersion (a few minutes) resulted in higher BSA adsorption on Cr than on Mo; for longer times (20 min, 1 h), the amount of BSA was similar on both surfaces. Changes in the conformation of the BSA molecules when the coverage increases were evidenced by the position and shape of the IR amide band. A more compact structure was observed on chromium. On molybdenum, the amideI/amide II intensity ratio did not change significantly with time or BSA concentration, indicating limited change in the conformation upon adsorption. In a Na_2HPO_4 + NaH_2PO_4 buffer solution, both FT-IRRAS and XPS data show that the amount of proteins adsorbed is reduced by a factor of close to three. Competitive adsorption of phosphates and proteins was inferred to explain this phenomenon.

Introduction

The interaction of proteins with metal and oxide surfaces has become a key issue in several areas, such as biocompatibility of materials used for implants or biofilm formation in food packaging or marine environments. A number of studies have recently been devoted to the characterization of protein layers on solid surfaces and tried to explain how an adsorbed protein layer affects the cell adhesion.[1−3] For these purposes, a combination of surface techniques, as well as more conventional biochemical techniques, have been applied. Proteins are complex molecules having hydrophilic and hydrophobic side chains and possibly undergo conformation changes upon adsorption leading to more strongly bound macromolecules. Adsorption of various proteins on metal surfaces was investigated in detail by Ishida and Griffiths, who demonstrated the role of the pH both on the rate of adsorption and on the structure of the adsorbed layer.[4] In fact, the role of the pH and of the ionic strength of the solution is already determined in solution. As an example, the diffusion of BSA in solution was shown to be divided by a factor 10 when passing from a deionized to a phosphate-buffered solution.[5] Consequences on the kinetics of adsorption may be expected from such an effect. The effect of pH on the conformation of BSA in aqueous solution was made clear by several authors using attenuated total reflectance Fourier-transform infrared (ATR-FT-IR) spectroscopy.[6,7] The shape of a globular protein in solution also depends on the ionic strength of the solvent because it sets the intermolecular forces, the salt molecules acting as screens between molecules (Derjaguin, Landau, Verwey, and Overbeek (DLVO) theory).[8] Salt-induced aggregation may hence occur in solution. The interaction of proteins with a solid surface also causes changes in their conformations, and this is of course related to the nature of the solution and to the physical and chemical properties of the substrate. A combination of several techniques is often applied to characterize the adsorption of proteins on solids. Radiolabeling, combined with X-ray photoelectron spectroscopy (XPS) and time-of-flight secondary-ion mass spectrometry (TOF-SIMS) enabled P. Bertrand and co-workers to determine the amount of fibronectin on a polystyrene surface and to characterize the layer structure.[9] In agreement with other authors, they concluded that the protein adsorbs following two stages corresponding to two different orientations of the molecule. The authors emphasized the influence of the substrate upon the coverage and conformation of the protein.

Adsorbed proteins were first observed by scanning tunneling microscopy (STM) by J. D. Andrade and co-workers[11] and more recently by atomic force microscopy (AFM) by Mori and Imae.[10] They proposed a scheme on mica involving changes in the orientation of the adsorbed BSA molecules when the coverage increases.[10,11] Interestingly, the kinetics of adsorption was also found to be dependent on the pH of the solution in a complex way; positively charged BSA initially adsorbs rapidly on mica that bears negative charges in a strongly acidic solution, pH 3 (the isoelectric point of BSA is pH 4.7[12]); a single BSA monolayer is attained because of intermolecular electrostatic repulsion, whereas at pH 6, the affinity between BSA and the mica surface overcomes electrostatic repulsions resulting in multilayer adsorption. One may add that the ionic strength of the solvent may also affect the kinetics of adsorption via the diffusion rate of macromolecules in solution.

* To whom correspondence should be addressed. E-mail addresses: pradier@ext.jussieu.fr, pmarcus@ext.jussieu.fr.
† Ecole Nationale Supérieure de Chimie de Paris.
‡ Hungarian Academy of Sciences.

10.1021/jp026365i CCC: $25.00
Published on Web 06/19/2003

Recently, adsorption of BSA was studied on calcium phosphate and on titanium surfaces. Using FT-IR, the authors showed that the structure and the composition of the initial surface greatly influence the kinetics of protein adsorption and the structure of the adsorbed layer. These results are explained in terms of ionic and electrostatic interactions between proteins and surfaces, which result in a possible loss of the α-helical structure of the protein.[13] BSA in water has an ellipsoidal shape with a 116 Å long and 27 Å short axis,[14] and intramolecular disulfide bridges form three domains in the peptide chain.[15] As for other proteins, its structure can be reorganized to optimize its interaction with a solid surface. This was clearly demonstrated on calcium phosphate surfaces. Weaker adsorption and smaller conformational changes of BSA were observed on titanium.

The importance of electrostatic interactions has been emphasized in an investigation of BSA adsorption on clay surfaces by using FT-IR spectroscopy. On mineral substrates, important changes in the amide I and II band shapes were observed; they were ascribed to strong electrostatic interactions of the charged side chains of the protein with the surface that result in its unfolding and strong bonding.[16] The combined role of surface hydrophobicity and electrostatic interactions was exemplified for BSA on modified calcium hydroxyapatites [17] and, more generally, for globular proteins on solid surfaces. Changes of conformation are generally more important on hydrophobic than on hydrophilic surfaces, involving a higher amount of irreversibly bound macromolecules on the former type of substrates.[18,19] The electrostatic properties of the metal oxide, in particular the surface charge density, greatly affected the adsorption process of BSA; an explanation for that is the interaction of carboxyl groups of BSA molecules on either positively or negatively charged metal oxide surfaces.[20]

These few examples, drawn from a recent survey of the literature in the field, provide sufficient proof of the role of the type of solution and of the substrate upon the interactions between proteins in solution and with the surface that may condition the coverage and structure of the adsorbed layer. However, little is said about the role of the ionic components present in the saline solution used to dissolve the BSA.

The present study aims at comparing the BSA adsorption processes on two different metals, chromium and molybdenum, in two solutions, pure water and water with a phosphate buffer (pH 7). Cr and Mo were chosen because they are important alloying elements of stainless steels, which are commonly used materials in the food industry, in medical applications, and in marine environments. Characterizing the interaction of BSA with these materials is a key step toward the understanding and control of the process occurring when stainless steel surfaces are immersed in a liquid containing biomolecules. In a previous study, it was observed that chromium, covered with a natural oxide layer, exhibits a high reactivity toward BSA adsorption; [21] all immersion experiments had been carried out in a 0.01 M phosphate-buffered solution. In the present work, two aqueous solvents, pure water and phosphate buffer at 0.1 M, were used to determine the possible role of ions in solution in the adsorption process.

Among the various techniques currently used to investigate the adsorption of biomolecules on solid surfaces, FT-IR spectroscopy and X-ray photoelectron spectroscopy (XPS) are very sensitive to the amount of adsorbed proteins and additional information on the structure of the adsorbed layer can also be obtained by FT-IRRAS. Infrared spectroscopy was applied in the absorption−reflection mode (FT-IRRAS) at grazing angle to enhance the signal/noise ratio.

Materials and Methods

Substrates. The investigated materials were pure chromium and molybdenum samples (99.9%, 12 mm diameter) purchased from Goodfellow. Prior to immersion in the BSA solutions, the samples were mechanically polished with SiC paper, followed by diamond paste, down to 0.5 μm. Immediately before immersion in the solutions containing the protein, the chromium and molybdenum samples were cleaned in ethanol at room temperature, rinsed twice in bidistilled water at 50 °C, and dried with clean air.

BSA Adsorption. The BSA solutions were prepared by dilution of an initial BSA (Sigma) 100 mg/L stock solution down to 1, 5, and 20 mg/L into high-purity water (Millipore, milliQ) or into a 0.1 M phosphate buffer ($Na_2HPO_4 + NaH_2PO_4$, pH = 7). In the absence of buffer, the pH of the pure water remained in the range 8−8.4.

The samples were immersed in the BSA solutions for 2, 5, 20, or 60 min. Then they were rinsed by two 20 s immersions in high-purity water (Millipore, milliQ) and dried under a pure air flow. The surfaces were then analyzed by IRRAS and XPS.

IRRAS Measurements. Infrared characterization of the surface was carried out in a reflection mode at a grazing incidence (6°) using a Fourier transform infrared spectrometer (Nicolet, Magna 550) with a mercury cadmium telluride (MCT) wide band detector. A typical spectrum was obtained by averaging the signal of 800 scans at a resolution of 4 cm^{-1}. All spectra were ratioed against a background spectrum recorded on a sample that had been cleaned as above-mentioned. Three spectra were taken for each condition of adsorption.

XPS Analyses. The XPS analyses were performed with a VG ESCALAB Mk II spectrometer, using the Al Kα X-ray source (1486.6 eV). A 20 eV pass energy was applied for analyzing the following core level regions: Cr $2p_{3/2}$, Mo $3d_{3/2,5/2}$, O 1s, C 1s, S 2p, and N 1s. The binding energies were calibrated against the binding energy of Au $4f_{7/2}$ and Cu $2p_{3/2}$; with this calibration, the low-energy carbon peak, attributed to hydrocarbon contamination, was measured at 285.4 ± 0.1 eV. The sensitivity factors of the elements were taken from ref 22; the transmission factor was checked to be constant. In the fitting procedure, no constraint was applied to the initial binding energy values; the full width at half-maximum (fwhm) was set at 1.4 ± 0.2 eV for the carbon contributions and 1.6 ± 0.2 eV for the oxygen contributions with a Gaussian/Lorentzian ratio, G/L, equal to 80/20.

Results

FT-IRRAS Data. All IR spectra were recorded after the samples were rinsed and dried. We focus here on the 1400−2000 cm^{-1} region, where the amide vibrational modes appear.

Figure 1 shows this region for the chromium (panel a) and molybdenum (panel b) surfaces after immersion of the samples in an aqueous solution of 5 mg/L of BSA. The spectra were slightly smoothed, 5 points, to cancel all absorption due to residual gaseous water in the spectrometer. The spectra are quite similar, both in shape and in intensity, for the two substrates. The expected vibration modes, $\nu_{C=O}$ and ν_{C-N}, δ_{N-H}, centered at 1658 and 1545 cm^{-1}, respectively, are observed (amide I and amide II). These peptide-characteristic signals increase with time of immersion from 2 to 60 min. From the amide I intensity, it appears that the adsorption of BSA is slower on Mo than on Cr in the first period (2 min of immersion). The amount of adsorbed BSA is similar on the two metals after 20 min or 1 h of immersion. The amide I/II intensity ratio has also been calculated and is reported in Table 1. Note that the band with

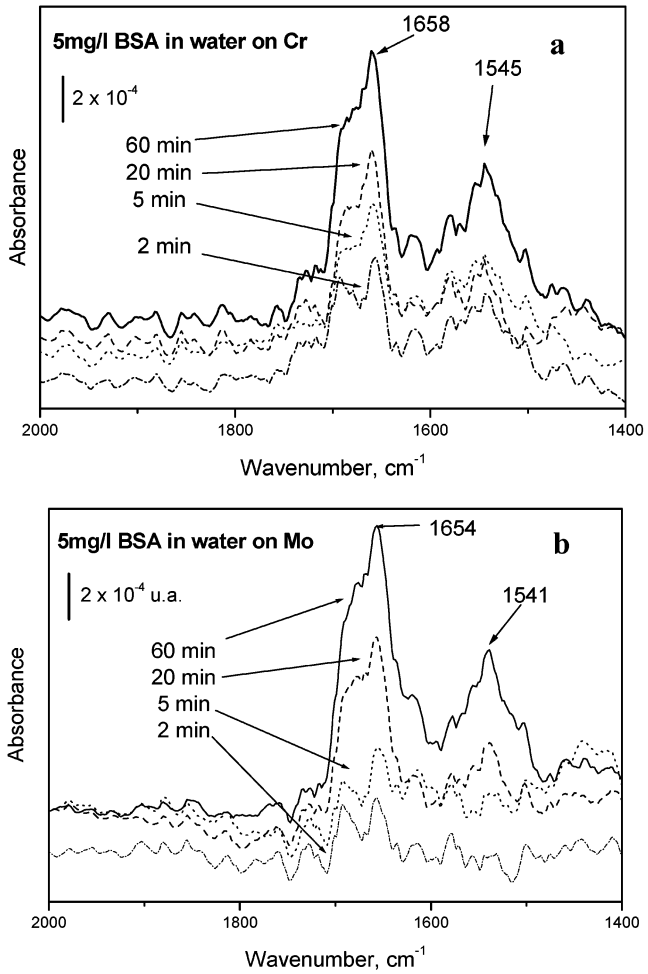

Figure 1. IRRAS spectra of the chromium and molybdenum surfaces after immersion in a 5 mg/L BSA−water solution for 2, 5, 20, and 60 min. The samples were rinsed and dried before analysis.

TABLE 1: Amide I/II Area Ratio and in the Amide I Band I′(1658 cm^{-1})/I″(1680 cm^{-1}) Area Ratio for Cr and for Mo after Immersion in 5 mg/L BSA−Water Solution

		time of immersion, min			
surface	ratio	2	5	20	60
Cr	amide I/II	1.3	1.4	2.5	1.7
	I′/I″	1.2	0.9	1.7	2.3
Mo	amide I/II	*a*	*a*	2.5	2.0
	I′/I″	1.0	1.2	1.1	1.1

[a] Very weak signals.

a maximum at 1658 cm^{-1} is broad and asymmetric. A curve fitting was made for the amide I band observed after immersion of both samples in a 5 mg/L BSA−water solution; an example of this band decomposition is presented, for Cr and Mo after 2 min of immersion, in Figure 2, panels a and b. The band could be fitted with two components at 1658 and 1680 cm^{-1}, and the ratio of the intensities of each component, labeled I′ and I″, respectively, is given in Table 1 for 2, 5, 20, and 60 min of immersion. An increase of both the amide I/II ratio and the I′/I″ ratio is observed on Cr when the time of immersion increases. Figure 3 presents, for Cr, the variations of the I′ and I″ contributions showing that the former, at 1658 cm^{-1}, is mainly responsible for the increase of the whole amide I signal.

By reference to the assignments established by several authors,[13,16,23−25] the high wavenumber contribution, 1680 cm^{-1}, is characteristic of β-turns and bends of partially unfolded BSA molecules,[26] whereas the one at 1658 cm^{-1} has been ascribed

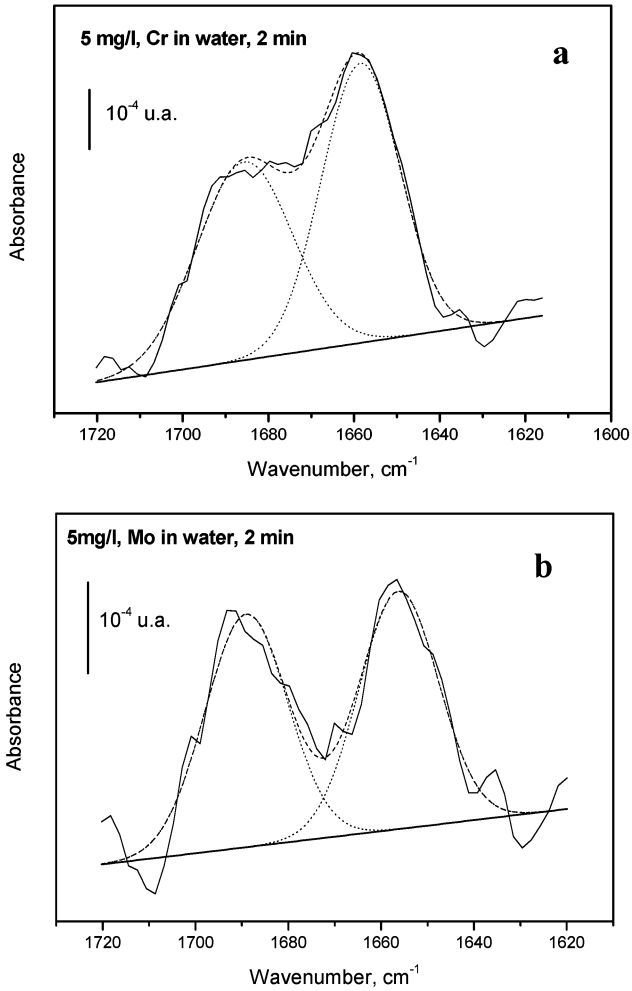

Figure 2. Decomposition of the amide I band for the Cr and Mo surface spectra after immersion in a BSA 5 mg/L solution for 2 min.

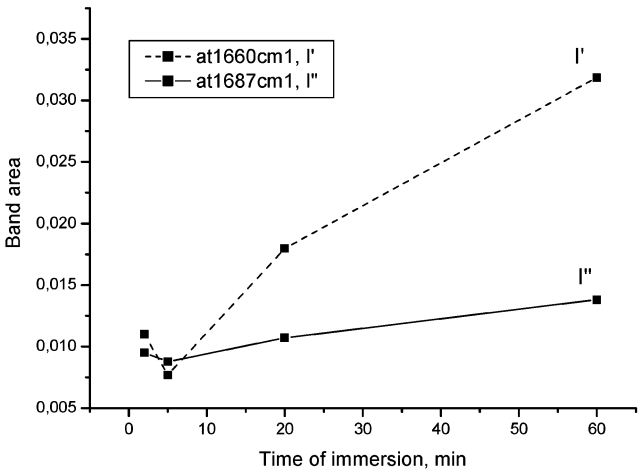

Figure 3. Variation of the areas of the 1660 and 1687 cm^{-1} contributions, I′ and I″, to the amide I band on Cr after immersion in a BSA 5 mg/L water solution.

to H-bonded CO in α-helixes and suggests the presence of packed hydrophobic helical domains. Considering that the peak components reflect the BSA conformation, a tendency to form dense packs of proteins on chromium is indicated by the relative increase of the lower wavenumber contribution with longer times of immersion. The increase in the I/II ratio brings an additional indication of some changes in the structure of the protein. A survey of the literature dealing with variations in the amide I/II

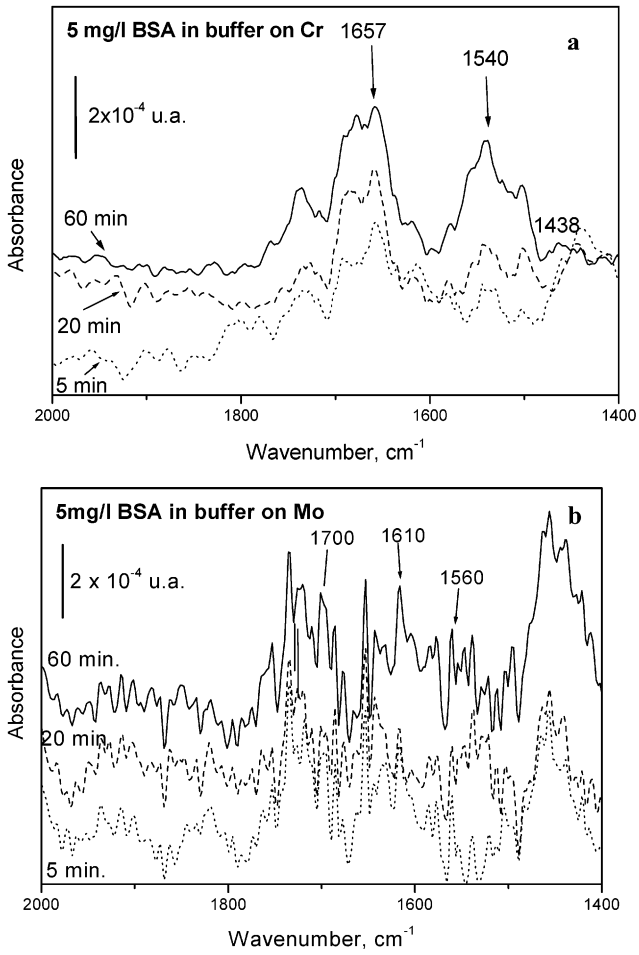

Figure 4. IRRAS spectra of the chromium and molybdenum surfaces after immersion in a 5 mg/L BSA−phosphate buffer solution for 5, 20, and 60 min. The samples were rinsed and dried before analysis.

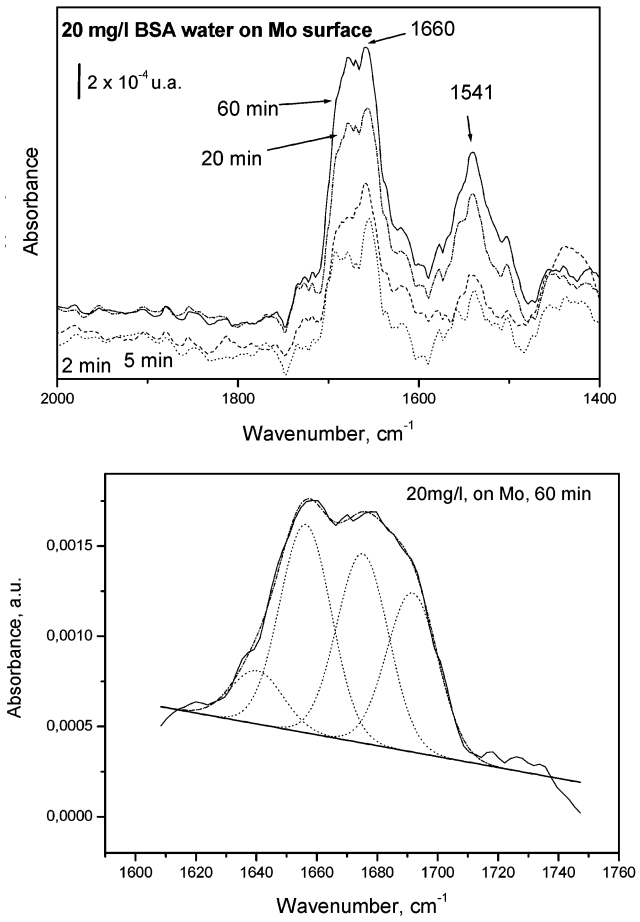

Figure 5. IRRAS spectra of the molybdenum surface after immersion in a 20 mg/L BSA−water solution for 2, 5, 20, and 60 min. The sample was rinsed and dried before analysis. Decomposition of the amide I band is shown for 60 min immersion.

ratio does not provide a clear correlation with the type of structural changes associated. It is however reported that, in the case of albumin in solutions of various pH, an increase of the helical domains of the protein is accompanied by an increase of the amide I/II ratio.[4,27]

On Mo, the evolution of the shape of the amide I band is much less marked than that on Cr, and the amide I/amide II ratio does not vary appreciably with time, suggesting limited changes in the conformation of the protein when the amount of adsorbed BSA increases. Note that, despite these differences in the peak shapes, the total amount of adsorbed protein, measured from the amide I intensity, seems to be similar on both substrates.

Significant differences were observed in the adsorption of BSA when a phosphate buffer was used. Adsorption of BSA from the phosphate buffer solution (pH 7) induces, both on Cr and on Mo, a strong decrease (factor ≈ 3) of the amide bands compared to the results observed in pure water (see Figure 4a,b). Moreover, after 5 min of immersion, the spectrum is dominated by a broad IR signal at 1080−1170 cm^{-1}(part of the spectrum not shown). The latter is ascribed to the P═O stretching mode of adsorbed phosphates, which clearly block the adsorption of BSA at the surface.

The concentration dependence of BSA adsorption was also tested on both Cr and Mo. From a 1 mg/L solution, a very small amount of BSA is present on the surface whatever the metal and the solvent. From a 20 mg/L solution, other parameters, metal and solvent, being identical, the adsorption of BSA was slightly more rapid compared to a 5 mg/L concentration and the amount adsorbed after 1 h of immersion was ∼20% higher. As an example, the spectra of the Mo surface after immersion in BSA, 20 mg/L in pure water, and the deconvoluted amide I band of the spectrum recorded after 60 min of immersion are displayed on Figure 5. Contributions at 1640 and 1675 cm^{-1}, which were absent on Figure 2, indicate the presence of BSA molecules in β-sheets, an ordered but less-dense structure than the α-helix one.[28]

Figure 6 summarizes the data, showing the intensity of the amide I band as a function of time of immersion for a 5 mg/L solution (Figure 6a) or as a function of BSA concentration after 60 min of immersion (Figure 6b) for the two metals and the two solvents.

XPS Data. Figure 7 shows the Cr $2p_{3/2}$, O 1s, C 1s, and N 1s XPS spectra of the chromium sample after 20 min of immersion in a 5 mg/L BSA solution in pure water. The same spectral regions, except for the metal peaks, were analyzed for the Mo sample; only the Mo 3d region is shown (Figure 7). The S 2p region was also recorded and exhibited a very weak peak on both metals (100−200 counts eV s^{-1}, spectrum not shown). The Cr $2p_{3/2}$, Mo $3d_{3/2, 5/2}$, O 1s, and C 1s peaks have been curved-fitted using the VG Eclipse software.

The Cr $2p_{3/2}$ peak was well-fitted with three components at 574.7, 576.7, and 578.3 eV corresponding to the metal, the oxide (Cr_2O_3), and the hydroxide ($Cr(OH)_3$), respectively. The chromium samples appear to be covered with a thin layer of oxide and hydroxide. Using values of the attenuation lengths calculated

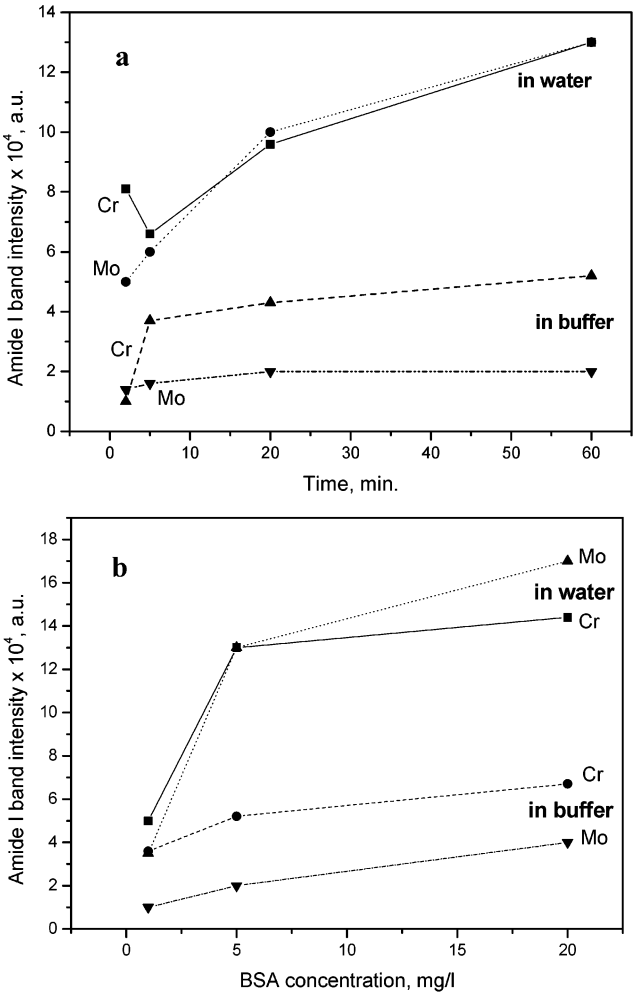

Figure 6. Variation of the amide I intensity (a) with time and (b) with BSA concentration on both metals in water or in buffer solutions.

from the Seah and Dench formula[29] and a model developed in ref 30 for the quantitative analysis of passive films on stainless steels by XPS, we calculated a thickness of 34 Å in agreement with other works.[31]

The Mo 3d spectrum was fitted with two doublets, a dominant one at 227.9/231.2 eV for the metal (Mo^0) and a weaker one at 229.1/232.6 eV for Mo^{4+}; the latter peaks were broad, probably including weak contributions from Mo hydroxide. There was no peak at ca. 232.4 eV indicating the absence of Mo^{6+} oxide, whatever the conditions of immersion.

The Mo surface is hence covered with a thin layer of MoO_2 oxide and possibly a small amount of hydroxide; a similar surface chemical state has been described in a previous paper.[30] After correction of the substrate intensities by the photoemission cross sections, calculated by Scofield for the Cr $2p_{3/2}$ and Mo $3d_{5/2}$ peaks, 7.69 and 5.62, respectively,[32] the Cr substrate appears slightly more attenuated by the organic layer than the Mo one for all conditions of immersion. Important is to note that, even after 60 min of immersion in BSA solutions, the metal signals were still intense (more than 10^5 counts s^{-1} eV).

The decomposition of the C 1s peaks was performed following the assignments of Rouxhet and co-workers.[33] An example is given in Figure 7 for the carbon spectrum recorded on chromium after 20 min of immersion in a BSA−pure water solution. The C 1s spectrum was fitted with four contributions: the first peak, at the lowest binding energy of 285.4 ± 0.2 eV, is assigned to carbon bound only to C or H; the second peak, at 286.5 ± 0.2 eV, is attributed to carbon in C−N and C−O single bonds; the third peak, at 287.8 ± 0.2 eV, is attributed to carbon in C═N or N−C═C groups; the fourth peak, at the highest binding energy of 288.8 ± 0.2 eV, is thought to include signals from carbon in CONH and COOH groups; the value of the BE for C 1s in COOH groups is slightly higher than that in ref 33 and is in agreement with other works.[34] The identified bonds correspond to the different chemical groups present in the BSA molecule. The highest binding energy peak is broad (fwhm = 1.85 eV) because it includes contributions from carbon in carboxylic or amide groups. This peak could also have been split into one contribution at 288.5 for the peptide groups and one at 288.9 eV for the acid groups, but only one broad peak was used for simplicity.

The number of carbon atoms in each type of chemical group was calculated from the various fragments of the protein[35] and compared to the XPS intensities, in percent, of each contribution; a good agreement was reached, providing evidence that chemically intact BSA molecules are adsorbed on the surface (see Table 2).

The O 1s spectra recorded on Cr and Mo surfaces were decomposed into three main components appearing at 530.7 ± 0.2, 531.7 ± 0.2, and 532.8 ± 0.2 eV. The absolute intensities are reported in Table 3. Their assignments were made by reference to literature data: the peak at 530.7 eV was attributed to oxygen from the chromium or molybdenum oxide layer[30] and possibly to oxygen in P═O groups; the one at 531.7 eV was attributed to oxygen in the OH of chromium hydroxide, in N−C═O bonds,[36] or possibly in adsorbed phosphate groups;[37] and a signal at 532.8 eV is assigned to oxygen atoms forming single bonds with carbon. The latter peak may also include a contribution from hydrated phosphate compounds [38] or phosphates bound to metal atoms.[39] The binding energy of the O 1s peak in phosphate components is indeed complex; according to certain works, oxygen atoms in P═O or $P-O^-$ bonds lead to a contribution at 530.5 and 531. 5 eV (with a C 1s peak set at 285.4 eV).[37,39,40]

Table 3 first confirms that the oxide layer is thinner on Mo than on Cr (first line). Second, the data indicate a slight decrease in the amount of organic material when passing from Cr to Mo after immersion in a BSA−water solution (second and third lines). Third, the presence of adsorbed phosphates, after immersion in a buffered solution, is likely to explain the increase of the three oxygen components; the amount of adsorbed phosphates seems to be lower on Mo than on Cr in agreement with the IRRAS data.

On Cr, the N 1s peak was symmetric, centered at 400.9 eV, as expected for the amine or amide groups of the protein.[41]

Table 4 presents the mole fractions of elements, excluding hydrogen, in the adsorbed organic material on the Cr surface. For the oxygen, the reported figures are the values obtained by subtracting from the total measured intensities the intensity expected to be due to the oxide/hydroxide, derived from the metal peak intensity. The numbers in columns 1 and 2 are in very good agreement with the elemental composition of BSA and confirm the presence of the macromolecule at the surface. Columns 3 and 4 indicate a large excess of oxygen that is easily explained by the presence of phosphates on the surface.

The N 1s peak was more difficult to measure on Mo because of its overlap with the Mo $3p_{1/2}$ level. For that reason, the calculation of the elemental surface composition was not done on that metal.

Finally, Table 5 reports the N/Cr or N/Mo molar ratios, calculated from the normalized XPS intensities, for 20 and 60

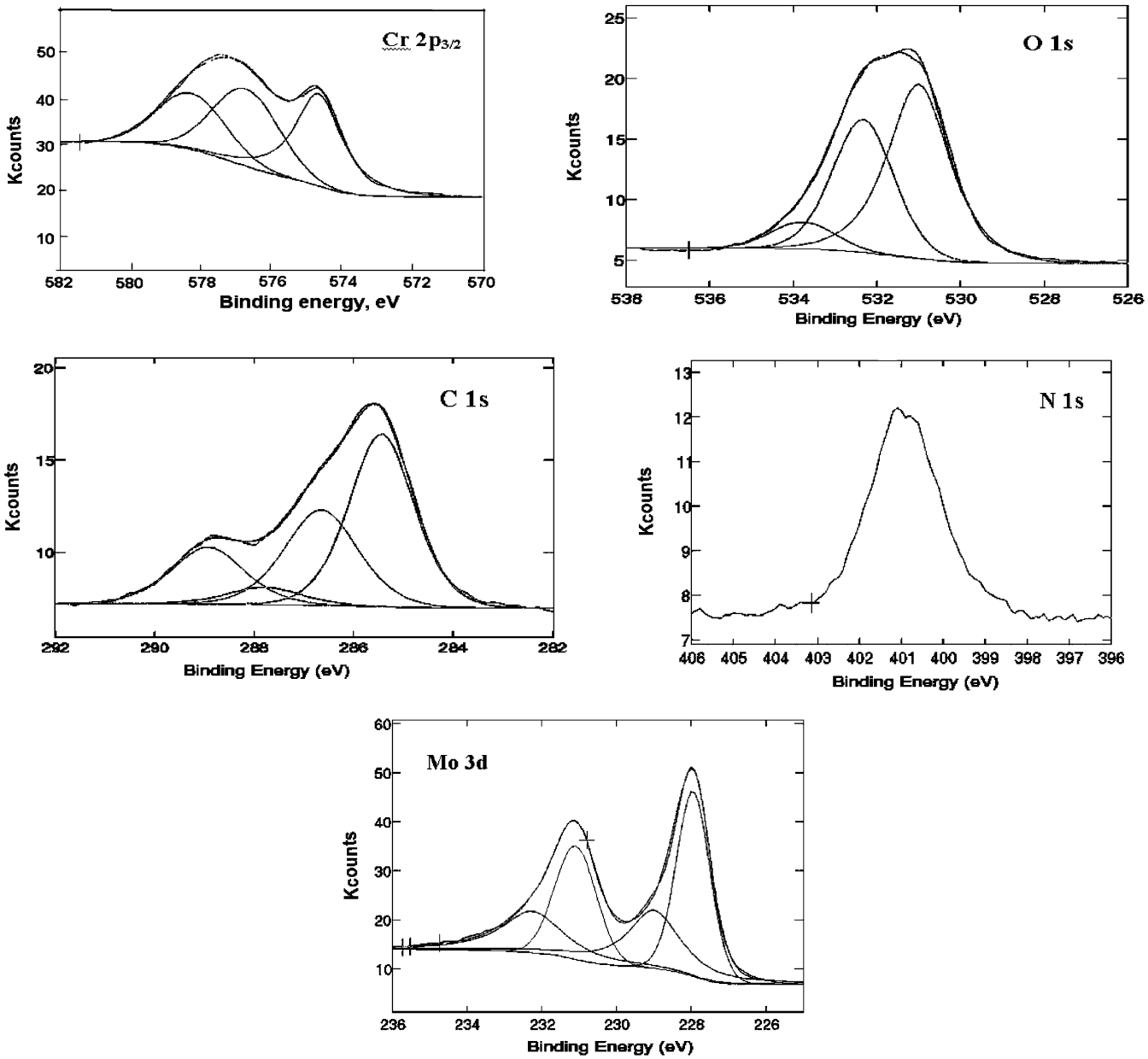

Figure 7. Cr $2p_{3/2}$, O 1s, C 1s, and N 1s measured on the chromium surface and Mo 3d of the molybdenum surface after 20 min of immersion in a 5 mg/L BSA−water solution. The samples were rinsed and dried before analysis.

TABLE 2: Comparison of the Fraction of Each Type of Carbon Atoms in the BSA Molecules to the Corresponding XPS Absolute Intensities (%) Measured on Cr after Immersion in a BSA Solution (20 mg/L, 20 min)

C type	no. of C type in BSA	% of C type in BSA	% of total C 1s peak intensity
C−C, C═C, C−H	1307	46	48
C−N, C−OH	793	28	30
C═N, N−C═C	74	2	4
COOH, CONH	705	24	18

TABLE 3: Absolute Intensities (Arbitrary Units) of the Components in the O 1s XPS Peaks on the Cr and Mo Surfaces after 20 min of Immersion in BSA Solutions

peak component (eV)	assignment	Cr, 20 min		Mo, 20 min	
		water	buffer	water	buffer
530.7 ± 0.2	O oxide, P═**O**	41 168	71 302	33 585	50 646
531.7 ± 0.2	OH, C**O**OH, NCO, PO_3^-, PO_4^{3-}	44 631	73 040	26 879	43 713
532.8 ± 0.2	C−**O**, metal−PO_4	23 230	33 618	13 432	17 666

min of immersion of both substrates in water or in the phosphate buffer (with 5 mg/L of BSA). Note that the N/Mo values are affected by some uncertainty due to the overlap of the N 1s and Mo 3p peaks. The P 2p peak intensity values after immersion in the phosphate-buffered solution are also given in Table 5.

The nitrogen to metal signal ratio does not vary significantly between 20 and 60 min of immersion whatever the solution, pure water or buffered solution. However, for identical times of immersion, the addition of phosphates to the solution induces a strong decrease (factor of 2−3) of the N 1s/metal peak intensity ratio, which suggests that adsorbed phosphates block the adsorption of BSA. Note also that the P 2p signal intensity indicates that the adsorption of phosphates is strongly favored on Cr compared to Mo without blocking the adsorption of BSA in the corresponding proportion.

TABLE 4: Surface Chemical Composition (Mole Fraction in %, excluding hydrogen) on Cr after Immersion in BSA Solutions and Mole Fraction in BSA

peak	20 min, water	60 min, water	20 min, buffer	60 min, buffer	% in BSA
O 1s	25	21.5	59	60	19
N 1s	10	10.7	5	4	17
C 1s	65	67	35	36	63
S 2p	0.2	0.3	<1	<1	<1

TABLE 5: XPS Data on Chromium and Molybdenum after Immersion in 5 mg/L of BSA in Pure Water and in Phosphate Buffer for 20 and 60 min

		pure water		phosphate buffer	
metal	peak	20 min	60 min	20 min	60 min
Cr	N 1s/ Cr 2p $_{3/2}$	0.34	0.32	0.12	0.11
Cr	P 2p			34 810	18 913
Mo	N 1s/ Mo 3d $_{5/2}$	0.2[a]	0.3[a]	0.1[a]	0.1[a]
Mo	P 2p			9953	11 230

[a] These values are affected by some uncertainty due to the overlap of the N 1s and Mo 3p peaks.

Discussion

Adsorption of BSA from aqueous solutions, pure water (pH 8.3), or water with phosphate buffer (pH 7), has been characterized by FT-IRRAS and XPS. The influence of concentration, time of immersion, nature of the metal, and solution on the amount of adsorbed BSA molecules will be first discussed. In a second part, possible changes in the protein layer structure when these parameters are varied will be examined.

After immersion in a pure water solution, the evolution with time of the amount of adsorbed BSA is similar on Cr and on Mo; after 60 min of interaction, no plateau was reached but the uptake of BSA was reduced compared to the shorter times of interaction. The XPS analysis suggests that the metals are not fully covered by a thick protein layer because a complete layer of BSA molecules would shield the metal to a larger extent than it does here (metal signals still intense); moreover, the BSA molecules are not decomposed upon adsorption. There is no, or very little, difference in the amount of adsorbed proteins on Cr and Mo when the BSA concentration varies from 5 to 20 mg/L. These data suggest that, although the surface is not totally covered, adsorption of BSA reaches a plateau, probably due to repulsive intermolecular interactions at a pH equal to 8, a significantly higher value than the protein IEP (4.8).[16]

This result is consistent with the calculated average separation distance between BSA molecules adsorbed on TiO_2, around 2 nm at pH different from the IEP and 0.5 nm at pH equal to the IEP.[42] Moreover, the same authors demonstrated that structural modifications of the adsorbed BSA molecules can be observed when BSA is adsorbed from aqueous media of various concentrations.[43] BSA molecules in a β-sheet structure are observed here together with α-helixes after immersion in a 20 mg/L solution (Figure 6), and this conformation, closer to the conformation of BSA in solution at high pH, suggests that the proteins undergo less unfolding and restructuring when adsorbed from a higher concentration solution.

After immersion in a phosphate-buffered solution, the amount of adsorbed proteins is severely reduced; this effect is clear both on the IRRAS spectra of Figure 4, summarized in Figure 6, and from the values of the N 1s/Cr 2p and N 1s/Mo 3d XPS intensity ratios (Table 5). This decrease could be attributed to the presence of phosphate compounds on the surface, evidenced both by FT-IRRAS and XPS. Higher quantities of phosphates, detected by XPS, were adsorbed on Mo compared to Cr for a similar decrease in the number of adsorbed proteins. This reveals that the effect of phosphate ions is more complex than a simple steric blocking of surface sites.

First, the pH varies from 8−8.4 to 7; this decrease modifies the charges born by the molecule and consequently reduces the intermolecular repulsive interactions. Second, according to the DLVO theory, the presence of ions in solution creates a barrier between molecules and the surfaces unfavorable to the adsorption.[44] The decrease with time of immersion in the amount of adsorbed phosphates on Cr, which is not compensated by a net increase in the BSA amount, confirms the role of the ionic strength of the solution in the adsorption process. This is also in good agreement with the recent work by Reyes et al.; they deduced from optical measurements that the BSA diffusion coefficient decreases by a factor 4 in a 0.1 M phosphate-buffered solution compared to pure water.[5] This is of course a kinetic parameter, which may explain the low rate of BSA adsorption from a phosphate-buffered solution (Figure 6).

IRRAS data provide additional information about the protein conformations. The amide I/amide II ratio indeed suggests that the structure of the macromolecules is dependent on the time of immersion and the nature of the substrate. One notes an increase in the fraction of molecules in an α-helix structure on Cr for longer times of immersion. No such tendency was observed on Mo suggesting that the structure of BSA is more compact on the former. We do not exclude that the drying step induces some structural changes in the adsorbed protein layer; however, previous in situ STM observations of BSA adsorbed on a chromium-enriched stainless steel surface revealed that the protein adopted in aqueous solution a compact and heterogeneous structure.[45]

The differences in the structures of the layers adsorbed on Cr and on Mo may find their origin in different types of interactions between BSA and the two metal substrates; a possible reason is the different levels of hydroxylation and charges of these two surfaces. In aqueous solution at pH in the range 7−8.3, both surfaces are presumably negatively charged,[46−48] and from our XPS data, Cr is totally covered with a hydroxide film, whereas Mo is only slightly hydroxylated. In the adsorption process, it is probable that the BSA internal structure is reorganized to optimize its interactions with the hydrophilic Cr oxide surface. Lu and Park also showed that the α-helix structure of BSA is favored on hydrophilic surfaces.[24]

Our data allow us to propose a sequential adsorption of BSA from an aqueous solution: when coming in contact with the metal surface, negatively charged BSA molecules undergo a partial unfolding to exhibit a maximal number of positive groups such as the N-terminal and lysine residue toward the surface.[49] It is indeed known that, even at pH > IEP, proteins still bear positive charges on their lateral chains and spontaneously adsorb on metal oxide surfaces even though the surface had the same charge.[20] This occurs both on Cr and on Mo during the first 20 min of immersion. Further adsorption of proteins tends to proceed so as to minimize the surface energy in two possible ways, either by occupancy of the free surface areas or by formation of a second layer of proteins on top of the already attached ones. The latter are probably less unfolded than the ones in contact with the surface and may adopt a more compact helical structure.[4] The helical domains of BSA are then formed by a gathering of the hydrophobic poles in the internal part of the protein. The former adsorption process prevails on Mo, whereas the latter predominantly occurs on Cr.

Conclusion

The adsorption of BSA on Cr and on Mo has been investigated by FT-IRRAS and XPS. A layer of adsorbed macromolecules is formed both on chromium and on molybdenum substrates.

Time dependency (0−60 min) and BSA concentration dependency (1, 5, and 20 mg/L) have been investigated. A rapid initial increase in the adsorbed BSA amount (0−5 min), followed by a slow uptake of macromolecules (20 and 60 min) was observed. The concentration dependence is characterized by a sharp increase from 0 to 5 mg/L (after 60 min) and almost a plateau for 5−20 mg/L.

The general features of BSA adsorption from pure water are very similar on Cr and Mo. However, the data show conformational changes of the BSA molecules that are different on the two substrates. The results suggest that the interactions between the negatively charged carboxylate groups (at pH > 4.7) or the positive side groups of the BSA and the passivated metal surfaces may be different on Cr and Mo.

Adsorption of BSA from a buffer solution (pH 7) severely reduces the amount of adsorbed BSA. This may be primarily ascribed to a site blocking by adsorbed phosphates. This blocking effect is more pronounced for Mo than for Cr. The increase in the ionic force of the solution may also reduce the electrostatic interactions between proteins and surfaces.

The combination of XPS and IRRAS techniques provided information on substrate- and solution-dependent BSA adsorption and gave evidence of the influence of adsorbed phosphates on the interaction of BSA on metals in aqueous solution.

References and Notes

(1) Busscher, H. J.; van Hoogmoed, C. G.; Geertesema-Doornbusch, G. I.; van der Kuijl-Booij, M.; van der Mei, H. C. *Appl. Environ. Microbiol.* **1997**, *10*, 3810−3817.

(2) Fletcher, M. *J. Gen. Microbiol.* **1976**, *94*, 400−404.

(3) Frolund, B.; Suci, P. A.; Langille, S.; Weiner, R. M.; Geesey, G. G. *Biofouling* **1996**, *10*, 17−30.

(4) Ishida, K. P.; Griffiths, P. R. *Appl. Spectrosc.* **1993**, *47*, 584−589.

(5) Reyes, L.; Bert, J.; Fornazero, J.; Cohen, R.; Heinrich, L. *Colloids Surf., B* **2002**, *25*, 99−108.

(6) Jakobsen, R. J.; Wasacz, F. M.; Brasch, J. W.; Smith, K. B. *Biopolymers* **1986**, *25*, 639−654.

(7) Qing, H.; Yanlin, H.; Fenlin, S.; Zuyi, T. *Spectrochim. Acta, A* **1996**, *52*, 1795−1800.

(8) Verwey, E. J. W.; Overbeck, J. T. G. *Theory of Stability of Liophobic Colloids*; Elsevier: Amsterdam, 1948.

(9) Lhoest, J. B.; Detrait, E.; Aguilar, P. V. d. B. d.; Bertrand, P. *J. Biomed. Mater. Res.* **1998**, *41*, 95−103.

(10) Mori, T.; Imae, Y. *Colloids Surf., B* **1997**, *9*, 31−36.

(11) Feng, L.; Hu, C. Z.; Andrade, J. D. *J. Colloid Interface Sci.* **1988**, *126*, 650.

(12) Gallinet, J.-P.; Gauthier-Manuel, B. *Colloids Surf.* **1992**, *68*, 189.

(13) Zeng, H.; Chittur, K. K.; Lacefield, W. R. *Biomaterials* **1999**, *20*, 377−384.

(14) Fitzpatrick, H.; Luckham, P. F.; Eriksen, S.; Hammond, L. *Colloids Surf.* **1992**, 43.

(15) Brown, J. R.; Shockley, P. *Lipid−Protein Interaction*; Wiley: New York, 1982; Vol. 1.

(16) Servagent-Noinville, S.; Revault, M.; Quiquampoix, H.; Baron, M.-H. *J. Colloid Interface Sci.* **2000**, *221*, 273−283.

(17) Kandori, K.; Mukai, M.; Fujiwara, A.; Yasukawa, A.; Ishikawa, T. *J. Colloid Interface Sci.* **1999**, *212*, 600−603.

(18) Marsh, R. J.; Jones, R. A. L.; Sferazza, M. *Colloids Surf., B* **2002**, *23*, 31−42.

(19) Norde, W. *Colloid Interface Sci.* **1990**, *29*, 267.

(20) Fukuzaki, S.; Urano, H.; Nagata, K. *J. Ferment. Bioeng.* **1996**, *81*, 163−167.

(21) Rubio, C.; Pradier, C. M.; Costa, D.; Bellon-Fontaine, M. N.; Relkin, P.; Marcus, P. *Colloids Surf., B* **2002**, *24*, 193−205.

(22) Briggs, D.; Seah, M. *Practical Surface Analysis by Auger and X-ray Photoelectron Spectroscopy*; John Wiley & sons: New York, 1984.

(23) Byler, D. M.; Susi, H. *Biopolymers* **1986**, *25*, 469.

(24) Lu, D. R.; Park, K. *J. Colloid Interface Sci.* **1991**, *144*, 271−282.

(25) Maruyama, T.; Katoh, S.; Nakajima, M.; Nabetani, H.; Abbott, T. P.; Shono, A.; Satoh, K. *J. Membrane Sci.* **2001**, *192*, 201−207.

(26) Haris, P. I.; Servecan, F. *J. Mol. Catal. B: Enzym.* **1999**, *7*, 207−221.

(27) Wasacz, F. M.; Olinger, J. M.; Jakobsen, R. J. *Biochemistry* **1987**, *26*, 1464.

(28) Jakobsen, R. J.; Wasacz, F. M. *Appl. Spectrosc.* **1990**, *44*, 1478.

(29) Seah, M. P.; Dench, W. A. *Surf. Interface Anal.* **1979**, *1*, 2.

(30) Vito, E. d.; Marcus, P. *Surf. Interface Anal.* **1992**, *19*, 403−408.

(31) Costa, D.; Yang, W. P.; Marcus, P. *Materials Science Forum*; Trans Tech publications: Aedermannsdorf, Switzerland, 1995; Vol. 185−188.

(32) Scofield, J. H. *J. Electron Spectrosc. Relat. Phenom.* **1976**, *8*, 129.

(33) Boonaert, C. J. P.; Dufrêne, Y. F.; Derclaye, S. R.; Rouxhet, P. G. *Colloids Surf., B* **2001**, *22*, 171−182.

(34) Troughton, E. B.; Bain, C. D.; Whitesides, G. M.; Nuzzo, R. G.; Allara, D. L.; Porter, M. D. *Langmuir* **1988**, *4*, 365−385.

(35) Peters, T. *Adv. Protein Chem.* **1985**, *37*, 161.

(36) Boonaert, C. J. P.; Rouxhet, P. G. *Appl. Environ. Microbiol.* **2000**, *66*, 2548−2554.

(37) Aramaki, K. *Corros. Sci.* **2003**, *45*, 199−210.

(38) Landis, W. J.; Martin, J. R. *J. Vac. Sci. Technol., A* **1984**, *2*, 1108.

(39) Brow, R. K.; Kirkpatrick, R. J.; Turner, G. L. *J. Am. Ceram. Soc.* **1990**, *73*, 2293−2300.

(40) Ahimou, F.; Boonaert, S. C. J. P.; Adriaensen, Y.; Jacques, P.; Thonart, P.; Paquot, M.; Rouxhet, P. G. *Biochim. Biophys. Acta* **2002**.

(41) Dufrene, Y. F.; Marchal, T. G.; Rouxhet, P. G. *Appl. Surf. Sci.* **1999**, *30*, 45.

(42) Giacomelli, C. E.; Avena, M. J.; Pauli, C. P. D. *J. Colloid Interface Sci.* **1997**, *188*, 387.

(43) Giacomelli, C. E.; Esplandiù, M. J.; Ortiz, P. I.; Avena, M. J.; Pauli, C. P. D. *J. Colloid Interface Sci.* **1999**, *218*, 404−411.

(44) Overbeck, J. T. G. *Colloid Science*; Elsevier: Amsterdam, 1952.

(45) Compere, C.; Bellon, M.-N.; Bertrand, P.; Costa, D.; Marcus, P. *Biofouling*, in press.

(46) Griebenow, K.; Kilbanov, A. M. *J. Am. Chem. Soc.* **1996**, *118*, 11696.

(47) Park, G. A.; Bruyn, P. L. d. *J. Phys. Chem.* **1962**, *66*, 967−972.

(48) Hu, H.; Wachs, I. E.; Bare, R. S. *J. Phys. Chem.* **1995**, *99*, 10897−10910.

(49) Arnebrant, T.; Ivarsson, B.; Larsson, K.; Lundström, I.; Nylander, T. *Prog. Colloid Polym. Sci.* **1985**, *70*, 62−66.